Effect of Dispersion Slope of Highly Nonlinear Fibre on The Performance of Self Phase Modulation Based 2R-Optical Regenerator

Salman Ghafoor and Periklis Petropoulos
School of ECS, Optoelectronics Research Center.
University of Southampton, SO17 1BJ, UK.
Email: sag1z07@ecs.soton.ac.uk

***Abstract*— In this paper we numerically investigate the effect of dispersion slope of the highly nonlinear fibre on the performance of Self Phase Modulation based 2R-optical regenerators. Our numerical study shows that the dispersion slope has a significant impact on the shape of the transfer function of the regenerator. The dispersion slope can therefore be used together with the dispersion value and the filter offset as an additional parameter to control the performance of the regenerator. It is also shown that a high dispersion slope can be beneficial in increasing the energy yield of the regenerator by a maximum of 23%. Dispersion slope is also helpful in reducing the effect of pulse-to-pulse overlapping in high bit-rate systems.**

I. Introduction

Among the various fibre-based regenerators that have been proposed for 2R all-optical signal regeneration, the one proposed by Mamyshev [1] is most researched because of its simplicity and effectiveness. The Mamyshev regenerator uses Self Phase Modulation (SPM) to induce spectral broadening on the incoming signal and the broadened spectrum is then filtered at an offset wavelength to obtain a reshaped and re-amplified signal. It has been shown in [2] that this setup is very useful in providing efficient BER improvement in the case of ON-OFF Keying (OOK) signal transmission. Use of the regenerator with Phase Shift Keyed (PSK) transmission systems has also been investigated in [3] and [4]. In [3], the Mamyshev regenerator is used to perform 3R All-Optical regeneration on DPSK signals at 40 Gbit/s. The DPSK signal is first demodulated to OOK signal by a delay interferometer. The OOK signal is then amplitude regenerated using the Mamyshev regenerator. DPSK signal is again achieved by phase modulating a local optical clock signal with the regenerated OOK signal. Using this approach, it has been shown in [3] that apart from amplitude regeneration, significant phase regeneration is also achieved. Based on similar technique, All-Optical regeneration of RZ-DQPSK signal at 160 Gbit/s (80 Gsymbols/s) has been shown in [4]. Much of the research done on the physical structure of the regenerator has focussed on the properties of the highly nonlinear fibre (HNLF) to obtain optimum performance from the regenerator [5], [6], [7] and [8]. References [9] and [10] present generalized scaling rules which can be used to obtain optimum regeneration performance out of HNLFs with known parameters. These rules are presented in the form of a contour map that relates the values of different physical parameters of the HNLF and input signal to the output that is expected from the regenerator. In [11], the possibility of using multi-segmented fibre assemblies has been studied. However, all theoretical and numerical studies so far have considered a flat dispersion slope for the HNLF used in the regenerator. In this paper we will observe in detail the effect of varying dispersion slope of the HNLF on the performance of the regenerator.

II. Regeneration Setup

The setup considered in our numerical study is that of a typical Mamyshev regenerator and is shown in Figure 1(a) below.

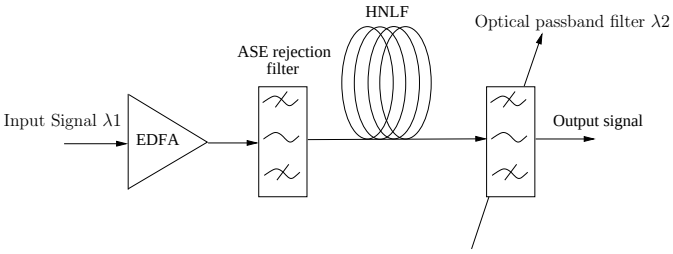

(a)

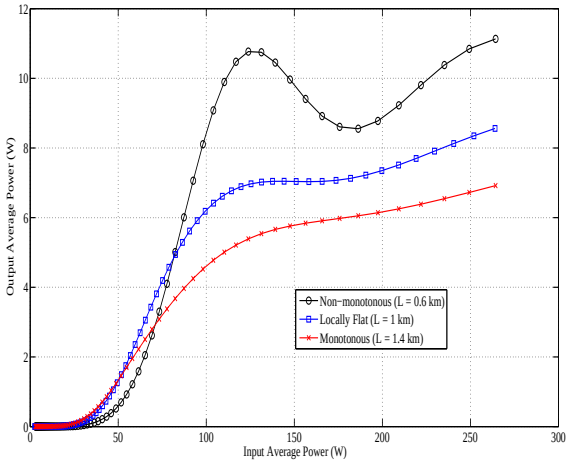

(b)

Fig. 1. (a) Schematic of a typical Mamyshev regenerator [1]. (b) Three types of transfer functions obtained by varying the length of HNLF.

The input signal consists of 10GHz Gaussian pulses having a pulse width of 6ps. The signal is first amplified through an erbium-doped fibre amplifier (EDFA), passed through an amplified spontaneous emission (ASE) rejection filter having a bandwidth of 1 nm and is then spectrally broadened by action of SPM in a HNLF which exhibits normal dispersion (-1.7 ps.nm^{-1}.km^{-1}) at the signal wavelength of 1545nm. The attenuation of the HNLF is 2.1dB/km and its nonlinearity

coefficient is 18 $W^{-1}.km^{-1}$. Initially we have assumed a dispersion slope value of 0.023 $ps.nm^{-2}.km^{-1}$, which is considered typical for commercial germanium-doped HNLFs. This value is varied in the studies presented in the following stages of the paper. Signal regeneration is achieved by action of an optical band-pass filter which is placed immediately after the HNLF and carves into the broadened spectrum at an offset wavelength relative to that of the input signal (in our case the filter position is at a shorter wavelength relative to the central wavelength of the input signal and 3nm away from it). The filter has a Gaussian response and a 3-dB bandwidth of 0.57nm which ensures that the pulses at the output have a similar width to those at the input.

As described in [9], depending upon the physical parameters of the regenerator and the spectral position of the filter, the transfer function (TF) shape will vary and can be classified into three main types. Figure 1(b) shows the three types of TFs which include a TF having a non-monotonous shape, another with a locally flat region which is considered optimum for regeneration, and finally one with a monotonous response. These TFs have been obtained by varying the length of the HNLF while keeping the rest of the parameters of the fibre unchanged. The lengths of HNLF used to obtain the non-monotonous, locally flat and monotonous transfer functions are 0.6 km, 1 km and 1.4 km respectively. In the next section, we discuss how a change in dispersion slope of the HNLF will vary the behaviour of the regenerator.

III. Effect of Dispersion Slope on SPM Based Regenerator

It can be seen from Figure 1(b) that the TF having a plateau region gives better compression of amplitude fluctuations on ones when the operating point is chosen at the middle of the plateau region. In order to observe how the signals after the HNLF for the three types of transfer functions shown in Figure 1(b) above look like, we have plotted the spectral and temporal shape of the signals after the HNLF as shown in Figure 2(a) and Figure 2(b) below.

The input average power used to obtain the plots in Figure 2(a) and 2(b) is 0.18 W which corresponds to the power at the middle of the plateau of the TF obtained with the 1-km long HNLF (see Figure 1(b)). It can be observed from Figure 2(a) and 2(b) that the temporal and spectral plots after the HNLF are slightly asymmetric. It will be shown later that this asymmetry is due to the small value of dispersion slope that we have used [12]. Also it can be noticed from Figure 2(b) that the spectral plots get flatter as we move from 0.6 km to 1.4 km. This flatness of the spectral top is responsible for the three types of transfer functions that are obtained from the regenerator [9] and [10]. We now observe how the spectral and temporal plots change when the dispersion slope of the HNLF is varied. The dispersion slope is varied by keeping the dispersion parameter constant at the signal wavelength while varying the rate of change of dispersion with the wavelength. In Figure 2(c) and 2(d) we have plotted the temporal and spectral profiles of pulses at the output of the HNLF by varying

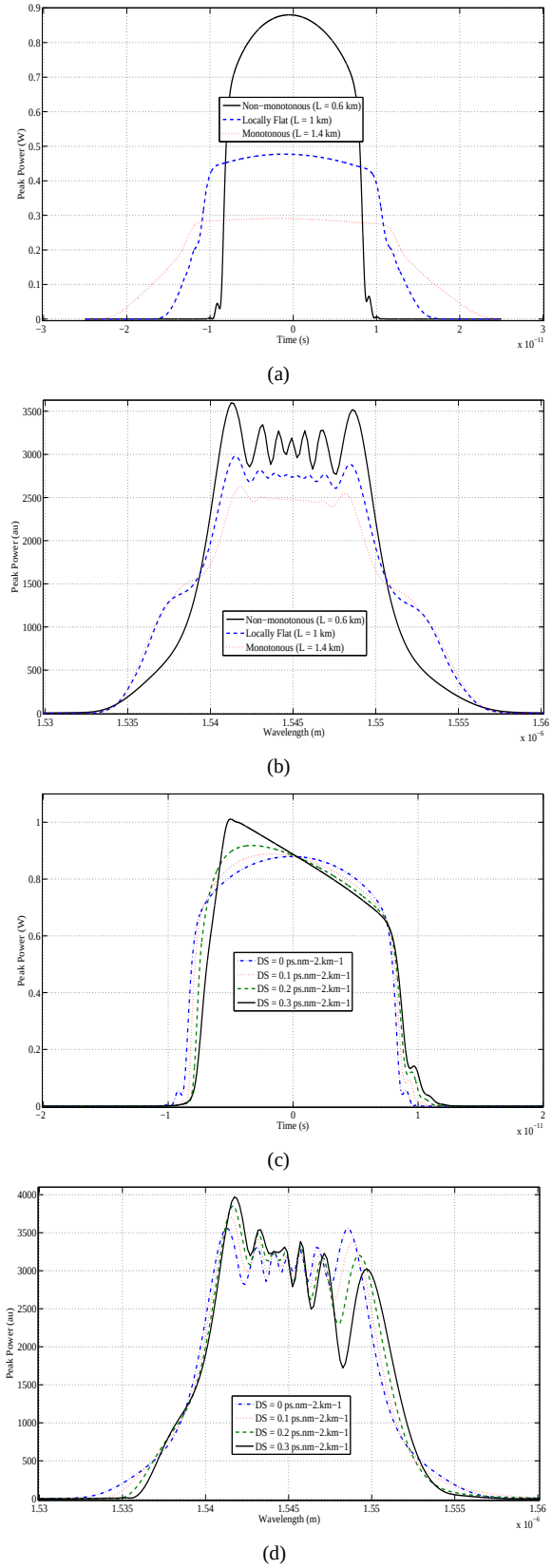

Fig. 2. (a) Temporal and (b) spectral plot of signals after HNLF for the three TFs shown in Figure 1(b). (c) Temporal and (d) spectral plot of signals after HNLF with varying dispersion slope.

its dispersion slope between 0 and 0.3ps.nm^{-2}.km^{-1}. It should be noted that these values of dispersion slope are rather high when considering step-index fibres but become relevant in the case of silica holey fibres, where it has been shown that appropriate control of the hole size and pitch can result in large values of dispersion slope, while maintaining a relatively high effective nonlinearity coefficient [13].

The input signal parameters used for the plots in Figure 2(c) and 2(d) are the same as those used in Figure 2(a) and 2(b) however, the length of HNLF is maintained in these cases at 0.6 km. As expected, an increase in the dispersion slope gives rise to an asymmetry in the power distribution of the broadened spectrum [12]. In addition, as the magnitude of dispersion slope increases, the side of the spectrum that corresponds to lower power components (longer wavelengths in Figure 2(d)) has more pronounced spectral lobes, whereas the spectral lobes on the opposite side (shorter wavelengths in Figure 2(d)) become less pronounced. This behaviour can be paralleled to the effect of changing the length of the HNLF as was shown in Figure 2(b), where the spectral lobes of the broadened spectrum become flatter as the length of HNLF is increased. The two effects are in fact related and result from the larger value of net dispersion at the wavelengths of observation. Therefore by keeping rest of the parameters of the regenerator constant, a variation in the dispersion slope of the HNLF should allow us to change the shape of the TF. It is worth mentioning here that similar conclusions can be drawn for dispersion slope values of sign opposite to the one used in Figure 2(c) and 2(d). The only difference in that case would be the asymmetry of the spectrum, which will now be opposite to that shown in Figure 2(b). In the next section we observe how this change in the dispersion slope affects the transfer functions of the regenerator shown in Figure 1(b) above.

A. Effect on non-monotonous transfer function

As shown in Figure 1(b), we obtain a non-monotonous TF when the HNLF has a length of 0.6 km, a dispersion of -1.7ps.nm^{-1}.km^{-1} at the signal wavelength and a dispersion slope of 0.023 ps.nm^{-2}.km^{-1}. Figure 3(a) below shows how the shape of the non-monotonous TF will vary with variation in the magnitude of dispersion slope.

In the plots shown in Figure 3(a), we increase the dispersion slope towards negative values. Therefore as discussed previously, this increase in the magnitude of dispersion slope will restrict the extent of spectral broadening on the long-wavelength side of the spectrum, thus making the spectral lobes flatter on that side. This in effect, tends to flatten the TF when the filter offset remains constant. Note that we focus on the top part of the transfer curve that is concerned with equalisation of ones, since a change in dispersion slope is not expected to have a significant effect on the suppression of the zeros. From Figure 3(a) it can be seen that the amplitude equalisation of ones improves with increasing the magnitude of dispersion slope, until the value of 0.17 ps.nm^{-2}.km^{-1} for which the TF exhibits a plateau region. With a further increase in the magnitude of dispersion slope, the TF moves towards a monotonous type and therefore the suppression of ones becomes worse. In Figure 3(a) the operating point on the TFs that gives minimum variation in the output signal for a variation in the input power of ones is also indicated. The input power at these operating points is called the nominal input average power in the remainder of the paper.

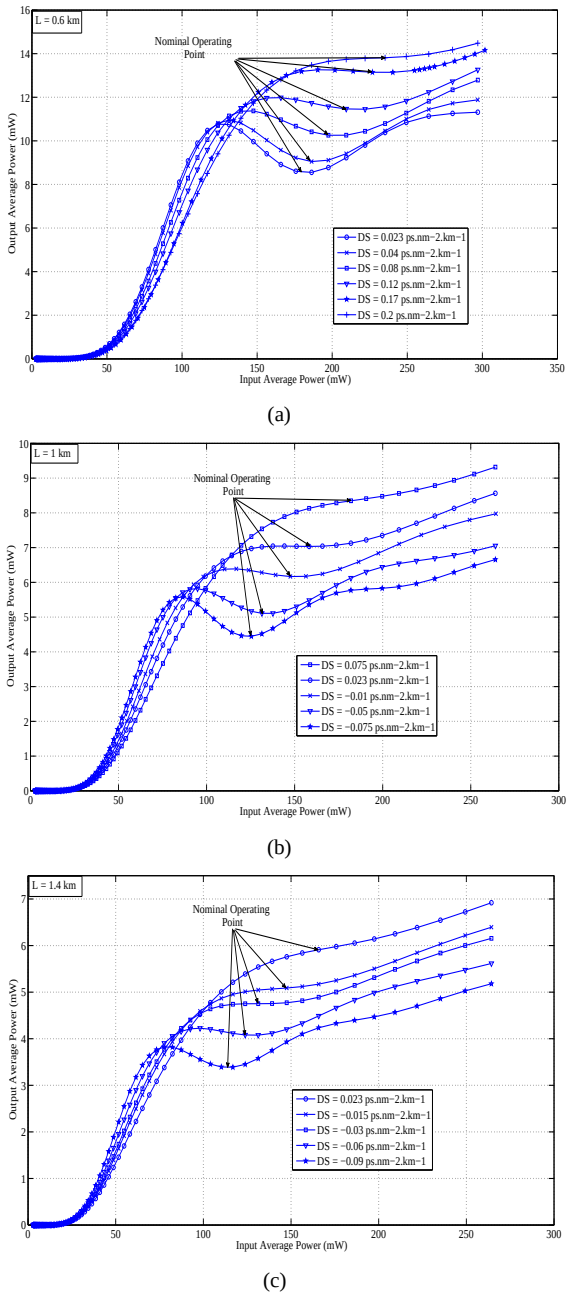

Fig. 3. Effect of varying dispersion slopes on the three types of TFs.

B. Effect on transfer function having a locally flat region

Next we consider the TF which has a plateau region. For the HNLF we have considered in our simulations, this occurs at a length of 1 km (Figure 1(b)). Figure 3(b) shows the effect of different values of dispersion slope on the shape of

this type of TF. It can be observed from the figure that as we increase the magnitude of the dispersion slope, the TF becomes either monotonous or non-monotonous, depending upon the sign of the dispersion slope. The reason for this variation in the transfer function is due to the variation in the shape of the broadened spectrum as mentioned earlier. Since the output offset filter is placed at the shorter wavelength side of the broadened spectrum, an increase in the magnitude of the dispersion slope flattens the spectral lobes on the shorter wavelength side, an effect similar to increasing the length of the HNLF. Therefore the transfer curve moves towards the monotonous type. The opposite happens when the dispersion slope is increased towards negative values.

C. *Effect on monotonous transfer function*

We obtain a monotonous TF when the HNLF considered in the simulations of Figure 1(b) has a length of 1.4 km. The effect of varying the magnitude of the dispersion slope in this TF is shown in Figure 3(c). It can be observed from the figure that the monotonous TF tends towards the one with a plateau region as the value of dispersion slope increases, whereas a further increase in the magnitude of the dispersion slope gives rise to a non-monotonic TF. For this to happen of course, the sign of dispersion slope needs to be opposite to that applied previously for the non-monotonous TF (see Figure 3(a)). The simulations shown in Figure 3 demonstrate that it is important to consider the effects of the dispersion slope in the system behaviour when HNLFs with a dispersion slope of a considerable magnitude are considered as can be the case of certain small-core holey fibre designs. This is true even for a wavelength offset of 3nm as is the case in the numerical simulations considered in this work.

IV. Effect on Energy Yield

As discussed earlier, when the value of dispersion slope is high, the spectral density of the nonlinearly generated frequency components on the two sides of the spectrum about the central wavelength is not equal. This effect is beneficial in the case of a relatively short HNLF which exhibits a locally flat TF by virtue of a high dispersion slope (as shown in Figure 3(a) above). This regenerator will exhibit an increased energy yield, since the filter is placed on the high-power side of the spectrum. Note that the energy yield is defined as the ratio of the power at the output of the filter to the power at the input of the HNLF [9]. In contrast, a relatively long HNLF with a high value of dispersion slope may exhibit a locally flat TF if the filter sits on the low-power part of the spectrum and the energy yield of the regenerator will therefore decrease. Figure 4 below summarises these findings by showing the variation in energy yield at nominal input average power versus dispersion slope for the TFs shown in Figure 3 above. The range of values used in Figure 4 are chosen in order to observe the effect of varying the sign and magnitude of dispersion slope on the energy yield of the three types of transfer functions shown in Figure 3 above.

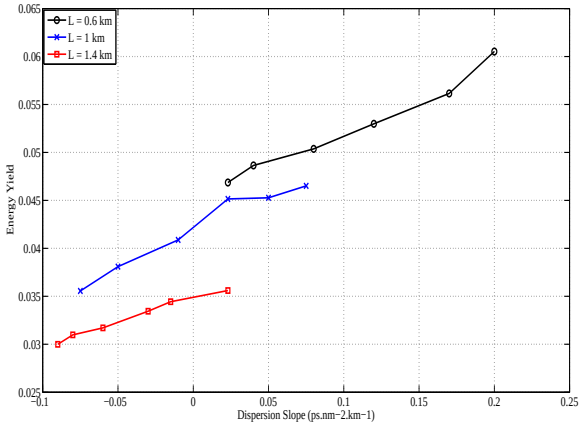

Fig. 4. Energy yield at nominal input average power as a function of the dispersion slope.

V. Reduction in Pulse-to-Pulse Overlapping

As discussed in [9] and [14], chromatic dispersion induced pulse broadening inside the HNLF causes the pulse to broaden to an extent that it overlaps with the adjacent pulse travelling along the fibre. We call this overlap of adjacent pulses inside the regenerator as pulse-to-pulse overlapping and it is a source of amplitude jitter at the output of the regenerator. The amplitude jitter increases with an increase in the bit rate of the system since the pulses become closer in time. It will be shown in this section that the effect of pulse-to-pulse overlapping can be reduced by suitably choosing the HNLF length and dispersion slope. For this purpose we consider the two transfer curves having a plateau region as shown in Figure 3(a) and 3(b). These TFs are obtained by using HNLFs of length 1 km and 0.6 km having dispersion slopes of 0.023 ps.nm^{-2}.km^{-1} and 0.17 ps.nm^{-2}.km^{-1} respectively. We choose these TFs since they provide maximum suppression of output power for a variation in the input power when operated at the nominal input power level. It can be observed from Figure 3(a) and 3(b) that the TF obtained for a high value of dispersion slope requires more power to operate at the plateau region as compared to the transfer curve obtained for a low value of dispersion slope. On the other hand, the energy yield of a regenerator based on a HNLF with a high value of dispersion slope is higher than that obtained when a low dispersion slope HNLF is used. Since pulse-to-pulse overlapping occurs inside the HNLF, we consider the pulse widths of the signals at the output of the HNLFs used to obtain the transfer curves shown in Figure 3(a) and 3(b) above. Figure 5 below shows the variation in the pulse widths at the output of the two HNLFs, plotted against a 20% variation from the nominal input peak power. In pulse-to-pulse overlapping it is the wings of the pulses that play a predominant role. Therefore their extent is of interest in this study. For this reason, we have chosen to plot the full pulse widths at 10% from the maximum in Figure 5, instead of full widths at half maximum. Also the peak powers are normalised with respect to the nominal input peak power (which is different for the two cases examined see Figure 3). For reference, Figure 5 also shows the bit duration for a 40 Gbit/s signal in order to

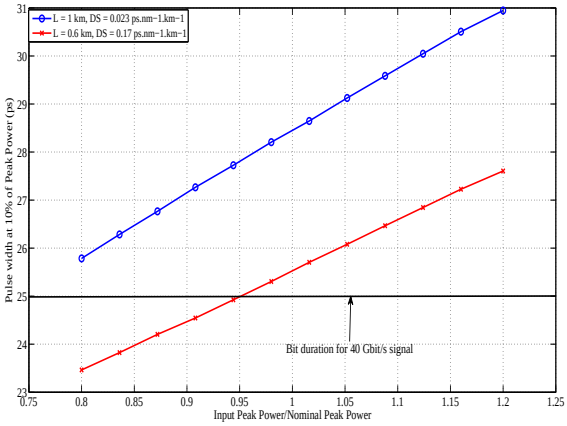

Fig. 5. Pulse width variation at the output of the HNLFs versus Input peak power variations for the two different HNLFs.

observe how pulse-to-pulse overlapping would affect a signal at this repetition rate (it is noted that the 6-ps pulses considered in this work are highly suitable for 40Gbit/s RZ systems). It can be observed from the figure that the pulse widths at the output of the HNLF exhibiting a high dispersion slope are significantly shorter than the corresponding of a HNLF with a low dispersion slope. Concluding, the effect of pulse-to-pulse overlapping for a regenerator using a short length, high dispersion slope HNLF will be less severe than for a regenerator based on a longer length HNLF exhibiting a low dispersion slope.

VI. Conclusions

We have presented a numerical study on the effect of the dispersion slope of an HNLF on the performance of a Mamyshev-type 2R regenerator. Our study reveals that with a change in the dispersion slope, the broadened spectrum after the HNLF becomes asymmetric and is accompanied by less pronounced spectral lobes on the side of the spectrum exhibiting a higher spectral density, while the opposite happens on the side corresponding to lower intensity spectral components. Depending on which side of the broadened spectrum the offset filter is placed at the output of the regenerator, the asymmetry changes the shape of the transfer function. Therefore HNLFs with similar optical properties at the wavelength of operation apart from the value of their dispersion slope yield markedly distinct regeneration performance. Also it should be noted that the shape of the transfer function can be varied by varying the offset wavelength of the output filter [9]. This property can be used to tune the performance characteristics of the regenerator if a fibre with the ideal values of dispersion cannot be made available. Some of the advantages of employing a high dispersion slope fibre in the regenerator include a higher energy yield and a higher resilience to pulse-to-pulse overlapping at high bit rates. Although the values of dispersion slopes used in our study are relatively high, such values are relevant in certain small-core silica holey fibre designs [13].

References

[1] P. V. Mamyshev, “All-optical data regeneration based on self-phase modulation effect,” *ECOC1998*, pp. 20–24, Sep 1998.

[2] M. Rochette, L. Fu, V. Ta‘eed, D. J. Moss and B. J. Eggleton, “2R Optical Regeneration: An All-Optical solution for BER Improvement,” *IEEE Journal of Selected Topics in Quantum Electronics*, vol. 12, pp. 736–744, July 2006.

[3] M. Matsumoto, “A Fiber-Based All-Optical 3R Regenerator for DPSK Signals,” *IEEE Photonics Technology Letters*, vol. 19, pp. 273–275, March 2007.

[4] M. Matsumoto, “All-optical DQPSK signal regeneration using 2R amplitude regenerators,” *IEEE Optics Express*, vol. 18, January 2010.

[5] T.-H. Her, G. Raybon and C. Headley, “Optimization of pulse regeneration at 40 Gb/s based on spectral filtering of self-phase modulation in fibre,” *IEEE Photonics Technology Letters* , vol. 16, pp. 200–202, 2004.

[6] P. Johannisson and M. Karlsson, “Characterisation of a Self Phase Modulation based all-optical regeneration system,” *IEEE Photonics Technology Letters*, vol. 17, pp. 2667–2669, Dec 2005.

[7] A. G. Striegler and B. Schmauss, “Analysis and Optimization of SPM-Based 2R Signal Regeneration at 40 Gb/s,” *IEEE Journal of Lightwave Technology*, vol. 24, pp. 2835–2843, Mar 2006.

[8] P. P. Baveja, D. N. Maywar and G. P. Agrawal, “Optimization of All-Optical 2R Regenerators operating at 40 Gb/s: Role of dispersion,” *IEEE Journal of Lightwave Technology*, vol. 27, pp. 3831–3836, Sep 2009.

[9] L. Provost, C. Finot, P. Petropoulos, K. Mukasa and D. J. Richardson, “Design scaling rules for 2R-optical self-phase modulation-based regenerators,” *IEEE Optics Express*, vol. 15, no. 8, pp. 5100–5113, 2007.

[10] L. Provost, C. Finot, K. Mukasa, P. Petropoulos and D. J. Richardson, “Generalisation and experimental validation of design rules for self-phase modulation based 2R-regenerator,” *OFC*, March 2007.

[11] L. Provost, C. Finot, P. Petropoulos and D. J. Richardson, “2R Regeneration Architectures Based on Multi-Segmented Fibres,” *ECOC 2008*, pp. 21–25, Sep 2008.

[12] T. Yamamoto, H. Kubota and S. Kawanishi, “Supercontinuum generation at 1.55 um in a dispersion-flattened polarization-maintaining photonic crystal fibre,” *IEEE Optics Express*, vol. 11, no. 13, pp. 1537–1540, 2003.

[13] F. Poletti, K. Furusawa, Z. Yusoff, N. G. R. Broderick and David J. Richardson, “Nonlinear tapered holey fibers with high stimulated Brillouin scattering threshold and controlled dispersion,” *IEEE Journal of Optical Society of America B*, vol. 24, Sep 2007.

[14] C. Finot, T. N. Nguyen, J. Fatome, T. Chartier, L. Bramerie, M. Gay, S. Pitois and J. C. Simon, “Numerical study of an optical regenerator exploiting self-phase modulation and spectral offset filtering at 40 Gbit/s,” *Optics Communications*, vol. 281, pp. 2252–2264, Dec 2008.